An algebraic solution for phase unwrapping problems in Multi-Wavelength Interferometry

Konstantinos Falaggis,[1] David P. Towers,[2] Catherine E. Towers,[2]

[1]*Institute of Micromechanics and Photonics, Warsaw University of Technology, 8Sw. A. Boboli St., 02-525 Warsaw, Poland*
[2]*School of Engineering, University of Warwick, Coventry. UK. CV4 7AL*

**Corresponding author: k.falaggis@mchtr.pw.edu.pl*

Received Month X, XXXX; revised Month X, XXXX; accepted Month X, XXXX; posted Month X, XXXX (Doc. ID XXXXX); published Month X, XXXX

Recent advances in multi-wavelength interferometry techniques (Falaggis et. al. Appl. Opt. 52, 5758–65 (2013)) give new insights to phase unwrapping problems and allow the fringe order information contained in the measured phase to be extracted with low computational effort. This work introduces an algebraic solution to the phase unwrapping problem that allows the direct calculation of the unknown integer fringe order. The procedure resembles beat-wavelength approaches, but provides greater flexibility in choosing the measurement wavelengths, a larger measurement range, and a higher robustness against noise, due to the ability to correct for errors during the calculation.

OCIS codes: 120.0120, 120.3180, 060.2370

http://dx.doi/org/10.1364/AO.99.099999

1. Introduction

A well-known problem with interferometry involves measuring an Optical Path Difference (OPD) larger than the source wavelength because of the ambiguity of the measured interferometer phase. Multi–wavelength interferometry (MWI) has been developed for a number of applications in the field of optical metrology to overcome this problem. Conventional [1] or extended [2–4] beat wavelength approaches increase the unambiguous measurement range (UMR) for a wide range of measurement wavelengths, however, these procedures do not always make use of the entire information contained in the measured phase [5,6]. Other methods such as the Chinese Remainder Theorem (CRT) [5,7–9], are restricted to particular sets of measurement wavelengths [5] and require in the presence of noise a partial least squares approach [6,9]. The method of Excess Fractions (EF) [6,10–12] provides high noise robustness, a high UMR, and full flexibility in choosing the measurement wavelengths [11,12]. However, a major drawback of the conventional EF approach is the time-consuming least square procedure to identify the correct integer fringe order. Recently [5,6,13], we have reported a unified theory of beat wavelength, EF and CRT approaches, which enables the derivation of a phase unwrapping method with low computational effort. Such a property had only been possible for CRT (for the case of no or very low noise [6]) and beat wavelength approaches. However, the approach presented in references [5,6,13] offers the flexibility in choosing the measurement wavelengths characteristic of EF in combination with a low computational effort. The results of that work can be used to determine the UMR, the measurement reliability and derive optimization criteria that are based on parameters that are in turn dependent on the choice of measurement wavelengths [11,12]. The model presented in references [5,6,13] provided a solution based on scaling and rotation matrices and gave a visualization with new insights to the behaviour of the phase unwrapping problem. This method directly calculates the integer fringe order for a series of N measurement wavelengths, where the measured phase values are used to compute a vector of size $(N-1)$ that contains the residual error components [6] using various matrices of size $(N-1)x(N-1)$ and associated exception handling. This procedure is optimal for single point absolute distance sensors because the matrix-vector multiplication can be implemented efficiently and in real-time on currently available Field Programmable Gate Arrays (FPGAs). However for full-field applications it is not desirable to generate a vector of size $(N-1)$ and carry out a series of matrix-vector multiplications for each pixel. There is clearly a need for a method that meets the memory requirement whilst providing a lower computational effort.

In this work an algebraic representation of the MWI phase unwrapping problem is presented that resembles the equations of beat-wavelength approaches – a representation that is well accepted within the optics community. Similar to the approach in [6], this procedure combines the flexibility and robustness of EF, but estimates the fringe order using a sequence of direct calculations. The approach derived here has a lower computational effort and lower memory requirements than the technique in [6], whilst giving a simple and intuitive calculation procedure without the need for exception handling that is currently only known for beat-wavelength approaches.

2. Algebraic Representation of the Phase Unwrapping Problem

Consider an MWI system with the measurement wavelengths λ_0, λ_1, λ_2, …, λ_{N-1} where N is the number of measurement wavelengths and ϕ_0, ϕ_1, ϕ_2, …, ϕ_{N-1}, are the corresponding measured values of the interferometer phase, which are found in the interval $[-\pi, \pi]$. A single optical fringe corresponds to the OPD of one wavelength, or to a phase difference of 2π. It is also possible to relate the measured interferometer phase ϕ_i that corresponds to the measurement wavelength λ_i to a so-called fractional fringe value ε_i defined as: $\varepsilon_i = \varphi_i / 2\pi$, where the possible values for ε_i are in the interval $[-0.5, 0.5]$. The relation between unknown integer fringe order m_i, fractional fringe value ε_i, and OPD for a set of N measurement wavelengths is given by:

$$OPD = u_i \lambda_i \tag{1}$$

where $u_i = m_i + \varepsilon_i$ is a dimensionless quantity and λ_i is a measurement wavelength with $\lambda_0 < \lambda_1 < \ldots < \lambda_{N-1}$. The relation between u_i and the fractional fringe value ε_i is given as: $\varepsilon_i = fract[u_i]$, where $fract(\cdot)$ is defined as the difference between a real value and its nearest integer $NINT(\cdot)$:

$$\mathrm{fract(x)} = \mathrm{x - NINT(x)}. \tag{2}$$

The complementary expression for the OPD that is related to a beat wavelength is given as

$$OPD = (M_{0i} + \mathrm{E}_{0i})\Lambda_{0i}, \tag{3}$$

where $M_{0i} = m_0 - m_i$, $E_{0i} = \varepsilon_0 - \varepsilon_i$, and Λ_{0i} is the beat wavelength of the measurement wavelengths λ_i and λ_0 calculated by [1]: $\Lambda_{0i} = sf_{0i}\,\lambda_0$, where $sf_{0i} = \lambda_i / (\lambda_i - \lambda_0)$, and $sf = sf_{0(N-1)}$. The calculation of the integer fringe order M_{01} requires several intermediate calculations. The first step requires the fringe information of the beat wavelengths Λ_{01} and Λ_{02} and is obtained via Eq. (3), i.e. using

$$(\mathrm{M}_{01} + \mathrm{E}_{01})\Lambda_{01} = (\mathrm{M}_{02} + \mathrm{E}_{02})\Lambda_{02}, \tag{4}$$

as

$$M_{01}F_{12} - M_{02} = \mathrm{E}_{02} - \mathrm{E}_{01}F_{12} \tag{5}$$

where $F_{ik} = \Lambda_{0i}/\Lambda_{0k}$. Eq. (5) also implies that the fractional part of the left hand side of Eq. (5) is equal to the fractional part of the right hand side of Eq. (5). Hence,

$$rem[M_{01}\, fract(F_{12})] = rem[\,\mathrm{E}_{02} - \mathrm{E}_{01}F_{12}\,] \tag{6}$$

so that

$$rem[M_{01}\, fract(F_{12})] = R_{1,2}(\mathrm{E}_{01}, \mathrm{E}_{02}) \tag{7}$$

with

$$\begin{aligned} R_{1,2}(\mathrm{E}_{01}, \mathrm{E}_{02}) &= rem[\,\mathrm{E}_{02} - \mathrm{E}_{01}F_{12}\,] \\ &= rem[\,\varepsilon_0(1 - F_{12}) - \varepsilon_2 + \varepsilon_1 F_{12}\,] \end{aligned} \tag{8}$$

where

$$\mathrm{rem(x)} = \mathrm{x - floor(x)}, \tag{9}$$

$floor(x)$ is the largest integer not exceeding x, and $fract(F_{12})$ can be developed with nearest integer continued fractions (NICF) [6,11-14] as

$$fract(F_{12}) \approx s_{k,12} / q_{k,12}. \tag{10}$$

The uncertainty due to noise in Eq. (8), is given as

$$\sigma_{Ri,j} = \sqrt{(1 - F_{i,j})^2 \sigma_{\varepsilon 0}^2 + (F_{i,j})^2 \sigma_{\varepsilon i}^2 + \sigma_{\varepsilon j}^2} \tag{11}$$

for the case of fully uncorrelated noise, and

$$\sigma_{Ri,j} = \sqrt{[(1 - F_{i,j})\sigma_{\varepsilon 0} + (F_{i,j})\sigma_{\varepsilon i} + \sigma_{\varepsilon j}]^2} \tag{12}$$

for the case of fully correlated noise, where $\sigma_{\varepsilon i}$ is the standard deviation of the noise in ε_i. The problem described in Eq. (7) shares similarities with the problem in Eq. (19) of reference [6]. Hence, the value of M_{01} can be solved similarly, provided the uncertainty in $R(E_{01}, E_{02})$ is sufficiently small. Notably, in addition to noise, the presence of any wavelength uncertainty has an effect on the number of NICF terms k in the rational approximation of Eq. (10) [11,12]. The individual beat wavelengths that are chosen for the calculation of M_{01} have to fulfil noise criteria (defined below) and need to provide sufficiently high wavelength accuracy such that the rational approximation in Eq. (10) can be maintained throughout the whole measurement. If these conditions are not met, it is necessary to limit the maximum value of k in Eq. (10) or to exclude those equations from the calculation of M_{01}, so they do not contribute to the extension of the measurement range. These cases may be particularly likely for large values of k in Eq. (10) or large values of F_{12}. In addition, wavelength uncertainty and interferometer dispersion affect the accuracy in the measured fractional fringe value ε_i and ultimately may limit the practically achievable UMR. A detailed analysis is presented in [12] for EF, but is directly applicable to the method of this work. The error probability p in the calculation step of Eq. (7) is given as

$$p = erfc\,[(q_{k,12}\, 2\sqrt{2}(\kappa + 6\sigma_{R_{1,2}(\mathrm{E}_{01}, \mathrm{E}_{02})}))^{-1}], \tag{13}$$

where $erfc(\cdot)$ is the complementary error function, and the parameter κ describes the error in Eq. (10) due to the NICF [6,11-14], with $\kappa \le 1/|q_k x_{k+1} + q_{k-1}|$, and $x_{k+1} = s_{k+1}/q_{k+1}$. Hence, following previous work, a noise criterion can be defined [5,6,11-13] to achieve a reliability larger than 99.73% (e.g more than 9973 out of 10000 measurements are correct) for the case in Eq. (7) as

$$1/q_{k,12} \ge \kappa + 6\sigma_{R_{1,2}(\mathrm{E}_{01}, \mathrm{E}_{02})}. \tag{14}$$

A graphical representation of the uncertainty present in Eq. (7), which can be used to derive Eq. (13), is shown in Fig. 1. It is based on the fact that possible solutions of $R_{1,2}(E_{01}, E_{02})$, can only have a value that is an integer multiple of $1/q_k$ [5,6]; hence, the errors generated by the phase noise and wavelength uncertainty must be sufficiently below this value. A measure of the reliability can be estimated statistically using Eqs. (11) to (13). Once a sufficiently high reliability can be ensured, a first estimate of M_{01} is given by [5,6,13]

$$M_{01}^{\#} = (NINT[R(\mathrm{E}_{01}, \mathrm{E}_{02})\, q_{k,12} W]) \bmod (q_{k,12}), \tag{15}$$

where W is a constant integer that fulfils $(W s_k) \bmod (q_k) = 1$. The estimated value of the fringe order $M^{\#}_{01}$ obtained through this calculation is related to the real value M_{01} as

$$M_{01} = M_{01}^{\#} + \mu_{12}\, q_{k,12} \tag{16}$$

where μ_{12} is an integer that describes the ambiguity of the value of M_{01}, i.e. $M^{\#}_{01} = (M_{01}) mod(q_{k,12})$. Hence, when using solely the equations for Λ_{01} and Λ_{02}, the *UMR* corresponds to the case with $\mu_{12} = 0$, so that $M_{01} = M^{\#}_{01}$. When comparing Eq. (15) to the phase unwrapping methodology reported by de Groot [2] (but applied to beat wavelengths rather than measurement wavelengths [3]), it is interesting to notice that Eq. (15) has the ability to extract more information and increase thereby the UMR. An interesting example that highlights this difference is depicted in Fig. 3 of reference [6], where the strategy in [2,3] is limited to $n \times \Delta_2 < \Delta_1$ with $n = 1, 2, 3$, etc.. Other phase retrieval techniques as EF [6,10-12], CRT based techniques [7–9], and other methods [4–6,13], reduce the ambiguity in M_{01} and thereby increase the UMR by utilizing the information in the remaining factional fringe orders. Here, this is accomplished by calculating the value of μ_{12} using $(M_{01}+E_{01})\Lambda_{01} = (M_{03}+E_{03})\Lambda_{03}$,

$$M_{01} F_{13} - M_{03} = \mathrm{E}_{03} - \mathrm{E}_{01} F_{13} \qquad (17)$$

so that an estimate for μ_{12} can be found as

$$rem[\,\mu_{12}\, q_{k,12}\, F_{13}\,] = rem[\,\mathrm{E}_{03} - \mathrm{E}_{01} F_{13} - M^{\#}_{01} F_{13}\,] \qquad (18)$$

such that

$$rem[\,\mu_{12}\;\; fract\,(q_{k,12}\, F_{13})\,] = R_{1,3}(\,\mathrm{E}_{01}, \mathrm{E}_{03}, M^{\#}_{01}) \qquad (19)$$

and

$$R_{1,3}(\,\mathrm{E}_{01}, \mathrm{E}_{03}, M^{\#}_{01}) = rem[\,\mathrm{E}_{03} - \mathrm{E}_{01} F_{13} - M^{\#}_{01} F_{13}\,], \qquad (20)$$

where $fract(q_{k12}\, F_{13})$ can be developed with NICF as

$$fract\,(q_{k,12}\, F_{13}) \approx s_{k,13} / q_{k,13} \qquad (21)$$

and a similar noise criterion can be defined as

$$1 / q_{k,13} \geq \kappa + 6\,\sigma_{R_{1,3}(\mathrm{E}_{01}, \mathrm{E}_{03}, M^{\#}_{01})}. \qquad (22)$$

As it was the case for the problem in Eq. (7), the parameter μ_{12} also exhibits a certain ambiguity,

$$\mu_{12} = \mu^{\#}_{12} + \mu_{13}\, q_{k,13} \qquad (23)$$

that is described with the parameter μ_{13}, i.e. $\mu^{\#}_{12} = (\mu_{12}) mod(q_{k,13})$. Hence, using Eqs. (15), (18), and (20), the integer fringe order M_{01} is given as

$$\begin{aligned} M_{01} &= M^{\#}_{01} + \mu_{12}\, q_{k,12} \\ &= M^{\#}_{01} + \mu^{\#}_{12}\, q_{k,12} + \mu_{13}\, q_{k,12}\, q_{k,13}. \end{aligned} \qquad (24)$$

Given the fact that $M^{\#}_{01}$, $\mu^{\#}_{12}$, $q_{k,12}$ and $q_{k,13}$ are known, the integer fringe order M_{01} is known if the UMR is limited to the possible values of M_{01} that correspond to the case where $\mu_{13} = 0$. When comparing the measurement range of Eq. (15) and (24) it becomes clear that M_{01} is unambiguously estimated within the interval $M_{01} = [0, q_{k12} - 1]$ and $M_{01} = [0, q_{k12}\, q_{k13} - 1]$, respectively. Hence, the calculation of the parameter $\mu^{\#}_{12}$ in Eq. (18) has increased the UMR of the interferometer. Similarly to the case of μ_{12}, the UMR can be further increased if the fringe information of any additional beat wavelengths is evaluated, using equations

$$\begin{aligned} M_{01} F_{1i} - M_{0i} &= \mathrm{E}_{0i} - \mathrm{E}_{01} F_{1i}, \\ M_{01}\, sf_{01} - m_0 &= \varepsilon_0 - \mathrm{E}_{01}\, sf_{01}. \end{aligned} \qquad (25)$$

It should be noted, that this procedure for determining M_{01} can formally only be used if the corresponding parameter F_{1i} has a fractional part and $fract(q_{k,1i-1} F_{1i}) \neq 0$. Moreover, the corresponding noise criterion:

$$1 / q_{k,1i} \geq \kappa_{k,1i} + 6\,\sigma_{R_{1,i}(\mathrm{E}_{01}, \mathrm{E}_{0i})} \qquad (26)$$

needs to fulfilled, where $q_{k,1i}$ is determined as

$$fract\,(q_{k,1(i-1)}\, F_{1i}) \approx s_{k,1i} / q_{k,1i}. \qquad (27)$$

Once the integer fringe order M_{01} is determined it is possible to calculate a first estimate of the integer fringe order M_{02}, using Eq. (5), of the next lower beat Λ_{02} as

$$M^{\#}_{02} = M_{01} F_{12} - (\mathrm{E}_{02} - \mathrm{E}_{01} F_{12}) \qquad (28)$$

and the ambiguity in M_{02} can be removed, similar to the case of Eqs. (15) and (22), using the fringe information of the remaining beat wavelengths

$$\begin{aligned} M_{02} F_{2i} - M_{0i} &= \mathrm{E}_{0i} - \mathrm{E}_{02} F_{2i} \\ M_{02}\, sf_{02} - m_0 &= \varepsilon_0 - \mathrm{E}_{02}\, sf_{02}. \end{aligned} \qquad (29)$$

Throughout this procedure, similar considerations that lead to Eqs. (25) and (26) have to be fulfilled. This procedure can also be applied in a similar manner for the remaining integer fringe orders $M_{03}, \ldots, M_{0(N-1)}$. Once the integer fringe order at the smallest beat-wavelength $M_{0(N-1)}$ is determined, the unknown fringe order of the smallest measurement wavelength m_0 is calculated as

$$rem(m_0 / sf) = rem(\mathrm{E}_{0(N-1)} - \varepsilon_0 / sf), \qquad (30)$$

using

$$fract(1 / sf) \approx s_{k,sf} / q_{k,sf}. \qquad (31)$$

3. Exemplary Case for Four Measurement Wavelengths

An example of this procedure is given for the case of four measurement wavelengths: $\lambda_0 = 1528$nm, $\lambda_1 = 1532.38698840832$nm, $\lambda_2 = 1542.98738907053$nm, and $\lambda_3 = 1597.4545454545$nm, giving $sf = 23$, $F_{23} = 94/21$, and $F_{12} = 95/28$. The integer fringe order at the largest beat wavelength M_{01} is calculated as

$$M_{01} = M^{\#}_{01} + \mu^{\#}_{12}\, q_{k,12}, \qquad (32)$$

where

$$\begin{aligned} M^{\#}_{01} &= (NINT[R(\,\mathrm{E}_{01}, \mathrm{E}_{02})\, q_{k,12} W_{M01}\,]) \bmod (q_{k,12}), \\ \mu^{\#}_{12} &= (NINT[R(\,\mathrm{E}_{01}, \mathrm{E}_{03}, M^{\#}_{01})\, q_{k,13} W_{\mu 12}\,]) \bmod (q_{k,13}). \end{aligned} \qquad (33)$$

The relevant coefficients for the calculation of M_{01} when using Eqs. (32) and (33) are given as

$$fract(F_{12}) = fract\left(\frac{95}{28}\right) = \frac{11}{28} \Rightarrow \begin{pmatrix} s_{k,12} = 11 \\ q_{k,12} = 28 \\ W_{M01} = 23 \end{pmatrix}$$

$$fract(q_{k,12} \cdot F_{13}) = fract\left(28 \cdot \frac{94}{21} \cdot \frac{95}{28}\right) = \frac{5}{21} \Rightarrow \begin{pmatrix} s_{k,13} = 5 \\ q_{k,13} = 21 \\ W_{\mu 12} = 17 \end{pmatrix}$$

$$fract(q_{k,12} \cdot q_{k,13} \cdot F_{13} \cdot sf) = 0.$$

Notably, because the parameter *sf* does not have a fractional part, it does not provide any information that extends the unambiguous range of M_{01}. Hence, $\mu^{\#}_{13}$ cannot be calculated. For the exemplary case of $OPD = 105300.1\,\lambda_0$, one would obtain $E_{01} = 0.4580$, $E_{02} = -0.1961$, $E_{03} = 0.2652$, and $\varepsilon_0 = 0.1$. The corresponding intermediate residual errors are obtained as

$$R(\mathrm{E}_{01}, \mathrm{E}_{02}) = -1.75,$$
$$R(\mathrm{E}_{01}, \mathrm{E}_{03}, M^{\#}_{01}) = -325.619.$$

Hence,

$$\begin{aligned} M^{\#}_{01} &= (NINT[R(\mathrm{E}_{01}, \mathrm{E}_{02})\, q_{k,12} W_{M01}]) \bmod (q_{k,12}) \\ &= (NINT[-1.75 \times 28 \times 23]) \bmod (28) \;= 21, \\ \mu^{\#}_{12} &= (NINT[R(\mathrm{E}_{01}, \mathrm{E}_{03}, M^{\#}_{01})\, q_{k,13} W_{\mu 12}]) \bmod (q_{k,13}) \\ &= (NINT[-325.619 \times 21 \times 17]) \bmod (21) = 10, \end{aligned}$$

and $M_{01} = M^{\#}_{01} + \mu^{\#}_{12}\, q_{k,12} = 21 + 10 \times 28 = 301$. The calculated value of M_{01} can be used for the calculation of $M^{\#}_{02}$ using Eq. (3), as

$$M^{\#}_{02} = (M_{01} + E_{01}) F_{12} - E_{02} = (301 + 0.4580) \times 95/28 - (-0.1961) = 1023.$$

The information at the other beat-wavelength can be extracted using

$$fract(F_{23}) = fract\left(\frac{94}{21}\right) = \frac{10}{21} \Rightarrow \begin{pmatrix} s_{k,23} = 10 \\ q_{k,23} = 21 \\ W_{\mu 23} = 19 \end{pmatrix}$$

$$fract(q_{k,23} \cdot F_{23}\, sf) = 0,$$

$$\begin{aligned} \mu^{\#}_{23} &= (NINT[R(\mathrm{E}_{02}, \mathrm{E}_{03}, M^{\#}_{02})\, q_{k,23} W_{\mu 23}]) \bmod (q_{k,23}) \\ &= (NINT[-4578 \times 21 \times 19]) \bmod (21) \\ &= 0, \end{aligned}$$

and $M_{02} = M^{\#}_{02} + \mu^{\#}_{23}\, q_{k,23} = 1023$.

Notably, for the example presented here, $\mu^{\#}_{23}$ always evaluates to $\mu^{\#}_{23} = 0$. However, in the presence of noise, there may be an error introduced in the calculation of M_{01}. The redundancy in these equations allows the correction of such errors when evaluating $\mu^{\#}_{23}$. The remaining integer fringe orders M_{03} and m_0 can be calculated directly using Eq. (1) and (3) (because $fract(sf) = 0$) as $M_{03} = (M_{02} + E_{02}) F_{23} - E_{03} = 4578$, and $m_0 = (M_{03} + E_{03}) sf - \varepsilon_0 = 105300$. A comparison to other algebraic phase unwrapping techniques is shown in Fig. 2a. Classical beat wavelength algorithms [1] are limited by the largest beat wavelength $UMR \leq sf_{01} \times \lambda_0$, and have a potential UMR equal to UMR = floor(349.303) λ_0=349λ_0. The extended beat wavelength algorithm reported by de Groot [2] uses the fractional part of the beat and has a potential UMR equal to UMR = floor(349.303/|fract(349.303)|)=1153 λ_0, but a high reliability can only be ensured [11,12] for UMR=1048 λ_0. The UMR of EF methods [10] are limited by wavelength coincidence, and therefore can be estimated to be equal to UMR = 23×95×94 λ_0= 205390 λ_0. The approach presented here, has the same UMR as EF and is equal to the distance where wavelength coincidence occurs. Fig. 2b. shows the simulated reliability for this approach for the case of Fig. 2a for each individual value for m_0, where a total number of 10000 simulations have been carried out for each value of m_0 having uncorrelated additive white Gaussian phase noise (AWGPN) of a standard deviation of 1/600th of a fringe. This highlights an interesting aspect of this method: one would expect that the example in Fig. 2 has to fulfil the noise criterion of Eq. (22) $6\,\sigma_{R1,3} \leq 1/q_{k1,3}$, which however cannot be fulfilled for a phase noise with a standard deviation of 1/600th of a fringe. Notably, the other residual error terms have the ability to correct for such deficiencies, and it is possible to show that a high reliability can be ensured - one that matches the performance of EF [6]. Such a property is not known for beat wavelength approaches. In EF, the individual residual error terms may be below the noise floor, but the necessary condition is that the sum of all individual residual error components are above the noise floor, i.e. in an EF solution the grid separation of points is sufficiently large [6,11,12]. Similar considerations apply to this work and explain the error correcting nature of this method. The overall reliability should therefore be estimated using the consideration in [6].

4. Experimental Verification

Experiments have been conducted using a fibre based MWI interferometer with fibre optical components that are operating in the C and L bands. The choice of this wavelength-range allows the exploitation of the wide variety of optical components available from the telecommunications market giving the opportunity to design a high specification but still cost-effective MWI interferometer. Commercially available Fiber Bragg gratings (FBGs) were used as frequency selection elements for C-band wavelengths in conjunction with erbium doped fiber amplifiers (EDFA) pumped at 980nm to achieve sufficient signal level. The FBGs used in this setup offer a bandwidth down to ~25 pm corresponding to a coherence length of > 90 mm, corresponding to > 117800 λ_0. The experimental setup is shown in Fig. 3. The wavelengths used for the experiments in Fig. 3 were: 1528.043, 1528.300, 1530.754 and 1595.289 nm. A broad band ASE source and FBG filters were used to reflect the 3 wavebands of interest in order to generate 3 C band wavelengths (1528 to 1531 nm).

These wavelengths are subsequently amplified by an EDFA. For the L band wavelength (1595.289nm) it was found that a higher power and narrower bandwidth could be obtained by placing the FBG in a fiber resonator containing a section of erbium doped fiber for amplification. The beams of the reference and measurement arm of the Michelson interferometer were collimated and sent free-space to mirrors with one mirror located on a linear traverse to adjust the optical path difference. One of the fiber arms of the interferometer contained a fiber wound cylindrical PZT and was driven by a sinusoidal waveform at 720Hz for phase modulation [15-17]. The main reason for the use of sinusoidal phase modulation techniques lies in the fact that they allow measurement of the phase at higher temporal bandwidths

and with a significantly increased accuracy in the phase shifter calibration giving a better phase accuracy. The return signals were sent to a de-multiplexer consisting of an array of FBGs and circulators to reflect individual wavelengths to photodiodes, see Fig. 3. This allowed the capture of the interference signal of each wavelength in parallel giving an increased robustness against interferometer instabilities [18]. The FBGs in the source and de-multiplexer for each measurement wavelength were matched to each other (within a few pm) and maintained at a constant wavelength by attaching the pair to a single Peltier based temperature controller. This allowed each measurement wavelength to be varied over a range of ~200 pm and for the power of the detected signal to be maintained across that range. The FBGs were sourced from O-E Land Inc. and had a reflectivity >50% and a bandwidth below ~20 pm.

Notably, if the separation between the measurement wavelengths is large (as it is the case here), it is also possible to employ FBGs with a larger bandwidth in the de-multiplexer unit giving a reduced effort in system optimisation, i.e. matching of the FBGs. For phase stepping analysis, a sinusoidal excitation of the PZT was performed [15-17] to avoid instabilities within the phase shifter itself and combined with algorithms to extract the required intensities at equal time steps, which results in a set of unequal phase steps among the measurement wavelengths. Here the procedure in [15] was used as it provides compensation for various error sources at each wavelength in the interferometer. A sequence of at least 50 wrapped phase values were obtained for each measurement wavelength at each optical path difference. This is done in order to verify the repeatability of the distance measurement.

The measurement wavelengths used in this setup form a series of beat wavelengths equal to Λ_{01} =9.09mm, Λ_{02} =862.80µm, Λ_{03} =36.25µm. Hence, with a conventional beat wavelength approach, the UMR is equal to the largest beat wavelength, i.e. UMR = Λ_{01}. However, the approach adopted here overcomes this limit. For the noise limit in this experiment, the maximum permitted value of q_k is $q_k \leq 45$: it can be shown that the approach of this work has a maximum UMR equal to UMR = 11894×λ_0 = 18.1745mm.

The performance of this set of wavelengths has been verified via simulation. The simulation results are depicted in Fig. 4 by the solid red curve and validate the predicted performance of this phase unwrapping procedure. For further validation, experiments have been carried out to verify this behaviour. The interferometer has been used to measure optical path differences from 0 to 21 mm, where the results illustrated in Fig. 4 (black squares) show an excellent match between the applied variation in optical path difference and that measured. The lower section of the figure shows a higher resolution set of data points with 20 µm between samples. The slight irregularity that can be observed is due to the resolution of the micrometer screw of the linear traverse used, which has a graduation of 10microns. However, the measurement results are free of outliers, which is a strong indication that there is neither a sensitivity to noise nor a failure of the error-correcting nature of this algorithm. The UMR can be seen to 'wrap' after 18.1745mm, which is exactly as predicted from both the developed model as well as the simulations in Fig. 4. The limitation of this fibre optical design lies in the wavelength stability in λ_i that is determined by the stability of the FBGs and the accuracy of the optical spectrum analyzer (OSA). A detailed analysis can be found in reference [12] (and is summarized in section 5); this indicates the tremendous improvement that can be made if the measurement wavelengths are extracted from a frequency-comb [19-21]. Nevertheless, in this configuration, a UMR of 2 multiples of the longest beat has been obtained. The phase noise in the measurements has been estimated at a standard deviation of 1/200th of a fringe, hence the overall dynamic range achieved is 1 part in 2.4×10^6.

5. Closing Remarks on Multi-Wavelength Interferometric Techniques

MWI techniques have a long tradition in Interferometry tracing back to the work of Benoit in 1898 [10]. The simplest form of MWI is a dual wavelength approach that forms a synthetic wavelength [1]. A drawback of synthetic wavelengths is given by the UMR that is limited by the largest beat wavelength, i.e. the separation between the two wavelengths. However, the information contained in the measured phase can be extracted to increase the UMR beyond the largest beat wavelength. Historically, this is accomplished using the conventional EF [10] approach, which evaluates all possible solutions of the unknown integer fringe order and hence the UMR. Indeed, if the ratio of the measurement wavelengths is irrational, the theoretically achievable UMR extends to infinity [11].

Nevertheless, in the presence of noise an infinitely long UMR cannot be achieved, because for a given measurement reliability the ratio of UMR / resolution has to be finite [11]. MWI techniques, allow this ratio to be increased by adding further measurement wavelengths. Early MWI approaches [22-24] form a series of synthetic wavelengths based on rules that form a geometric series. These so-called hierarchical approaches showed the possibility to extend the UMR exponentially with increasing numbers of measurement wavelengths. Hence, it would be theoretically possible to increase the UMR to very large distances (hundreds of km's) using less than ten measurement wavelengths.

However, there are a number of obstacles to be overcome (see section 5.1. and 5.2) before ultra-high dynamic range measurements can be made possible.

5.1. Wavelength Separation, Unambiguous Measurement Range, Computational Limits in Presence of Noise, and Interferometer Dispersion

The hierarchical approaches reported in [22-24] calculate the phase at a given synthetic wavelength and refine this OPD estimate using the phase information at the next smaller wavelength. A large UMR can only be achieved with very large beat wavelengths, which in turn results in very small wavelength separations. This however, requires a high system complexity and systems with larger wavelength separations have a lower UMR, if the integer fringe order is estimated using conventional beat-wavelength approaches.

Extended beat-wavelength approaches [2-4] tried to overcome this problem, by extending the measurement range beyond the largest beat wavelength. Such systems extend the UMR, or in other words, relax the requirements on the wavelength separations for a given UMR to be achieved. The essential problem with those types of solvers is that they do not extract the full information contained in the phase (see example in section 3), as they never match the performance of the conventional EF solver [10] for all sets of wavelengths.

The incentive regarding the efforts made in [5,6,13] and the approach presented in section 2 is to provide a deterministic phase unwrapping procedure with low computational effort that matches the performance of EF. In this sense, these methods enable revealing distance information that remain hidden in conventional or extended beat wavelength approaches. It should be noted, that these methods in [5,6,13] do not extract more distance information than EF, which is a least-square approach that evaluates the likelihood of all possible solutions. Nevertheless, being a deterministic method, these methods extract the same phase information with significantly lower computational effort.

Historically (and in absence of dispersion, refractive index and wavelength uncertainties), there was a computational limit (due to computational effort) to achieve a very large UMR (hundreds of km) with relatively few (less than ten) measurement wavelengths due to the presence of noise when having the requirements of rather large wavelength separations. The recent advances made in MWI algorithms ([5,6,13], this work) overcome this computational limit and match the performance of the EF least-square approach.

The previously described limits concerned the experimental needs of having rather large wavelength separations and the phase unwrapping procedure for a given level of uncertainty in the measured phase that is independent of the OPD. An analysis carried out in [12] discusses the presence of further error terms that are a result of changes in the measurement wavelength. A common practise in MWI is to take a reference phase measurement at a given distance and subtract these reference phase values from subsequent measurements. In this way, the phase at the reference position is nullified and all other measurements are calculated relative to the reference position. This is a crucial step in the presence of interferometer dispersion [12], because the fractional fringe order values contain the wavelength dependent offsets Δm_i and $\Delta\varepsilon_i$:

$$\varepsilon_i \mapsto \varepsilon_i + \Delta m_i + \Delta\varepsilon_i, \tag{34}$$

which can only be removed using a reference distance (or a virtual zero), OPD_{ref}, having:

$$\begin{aligned} OPD &= (m_i + \varepsilon_i + \Delta m_i + \Delta\varepsilon_i)\lambda_i \\ OPD_{ref} &= (m_{iref} + \varepsilon_{iref} + \Delta m_i + \Delta\varepsilon_i)\lambda_i. \end{aligned} \tag{35}$$

The reference location corresponds to a geometric location. Assuming ideal conditions the OPD relative to OPD_{ref} is given as:

$$OPD - OPD_{ref} = [(m_i - m_{iref}) + (\varepsilon_i - \varepsilon_{iref})]\lambda_i \tag{36}$$

However, in experimental practice, the measured fractional fringe orders of the actual OPD and OPD_{ref} do not correspond to the same measurement wavelength, because the measurement wavelengths may drift over time. Indeed, those changes in the wavelengths need to be accounted for when applying the subtraction in the fractional fringe values. When defining λ_i^* as the estimated (or measured) wavelength at the reference plane, and $\lambda_i^\#$ as the estimated wavelength at the actual OPD under test, it can be shown [12] that the resulting error is quantified as:

$$(\varepsilon_i^\# - \varepsilon_{iref}^\#) = fract\left[(\varepsilon_i^\# + \Delta\varepsilon_i^\#) - (\varepsilon_{iref}^* + \Delta\varepsilon_{iref}^*) - \frac{OPD_{ref}}{\Omega}\right], \tag{37}$$

where $(\varepsilon_i^* - \varepsilon_{iref}^*)$ is the measured fractional fringe order at the reference plane, $(\varepsilon_i^\# - \varepsilon_{iref}^\#)$ is measured fractional fringe order at the actual OPD, and the superscript # and * denote that the measurement wavelengths are subject to a wavelength uncertainty. The parameter Ω is a measure of the wavelength uncertainty of λ_i and is calculated as [12]:

$$\Omega = \frac{\lambda_i^* \lambda_i^\#}{\lambda_i^* - \lambda_i^\#}. \tag{38}$$

The parameter Ω is can be understood as a beat wavelength formed by the measurement wavelength at the actual OPD and the reference plane; for small wavelength uncertainties, Ω takes very large values. The accuracy in the estimated value of $(\varepsilon_i^\# - \varepsilon_{iref}^\#)$, which is used for the calculation of the fringe order in the algorithm, is degraded in addition to noise by the ability to measure Ω and OPD_{ref} accurately. Fortunately, most MWI systems can be designed such that OPD_{ref} is close to zero and the error in the measured fractional fringe orders of Eq. (37) (calculated as OPD_{ref}/Ω) is kept sufficiently small. It should be noted, that the error in Eq. (37), due to both wavelength uncertainty and interferometer dispersion is independent of the actual OPD to be measured, it poses the same computational limits as noise.

5.2. Uncertainty of the Refractive Index of the Medium and other Errors due to Uncertainties in the Measurement Wavelength

A more severe (and actually the most limiting factor) in ultra-high dynamic range measurements is an additional error term due to uncertainties in the measurement wavelengths and the refractive index of the medium (e.g. air) [12]. So far, we considered, without loss of generality, the case of MWI in a vacuum, where the reference OPD is degraded by dispersion, e.g. due to dispersive elements in the interferometer. However, for measurements in a medium (other than in a vacuum) the (wavelength dependent) ordinary refractive index should be used to determine each measurement wavelength in the medium and then the beat wavelengths determined [12], i.e

$$\lambda_i \mapsto \lambda_i / n_i \tag{39}$$

where n_i is the refractive index of the medium at λ_i. The wavelength in the medium can also be expressed using the optical frequency ν_i, *as* $\lambda_i = c/\nu_i/n_i$. The corresponding uncertainty in the measurement wavelength is therefore given as

$$\partial\lambda_i / \lambda_i = -\partial\nu_i / \nu_i - \partial n_i / n_i. \tag{40}$$

It should be noted however, that in most MWI phase unwrapping procedures, as e.g. EF, the actual accuracy of the individual measurement wavelength is of less importance as it is rather the changes in the beat wavelengths which are of greater concern. Recalling Eq. (8),

$$R_{1,2}(\mathrm{E}_{01}, \mathrm{E}_{02}) = rem[\,\mathrm{E}_{02} - \mathrm{E}_{01}F_{12}\,] \tag{41}$$

it becomes clear that similar considerations apply also to this work, because all quantities are related to beat wavelengths.

When following the considerations made in Eqs. (28) to (38) of [12], it can be shown that the error in $R_{1,2}$ is given as

$$\Delta R_{1,2}(\mathrm{E}_{01},\mathrm{E}_{02}) = |\, fract[U_{01}/S_{12}]\,|, \qquad (42)$$

where $U_{01} = M_{01} + E_{01}$ = OPD/Λ_{01}, and $S_{i,k}$ is a measure of the stability at the beat-wavelength, calculated as

$$S_{i,k} = F^{\#}_{i,k} F_{i,k} / (F^{\#}_{i,k} - F_{i,k}) \qquad (43)$$

where $F_{i,k}^{\#}$ is the value of $F_{i,k}$ with wavelength and refractive index uncertainties. With these additional wavelength uncertainties, to avoid unwrapping errors (outliers) a noise criterion similar to Eq. (26) must still be satisfied [12]:

$$1/q_{k,12} \geq |\, fract[U_{01}/S_{12}]\,| + \kappa_{k,12} + 6\sigma_{R_{1,2}}. \qquad (44)$$

Similar considerations apply also to the other residual error terms, which are used to evaluate the integer fringe order. If the noise criterion is not fulfilled and no error correction mechanism is successful, it may be necessary to reduce the maximum value of k in Eq. (10) or to exclude the equation from the calculation of M_{01}, so it does not contribute to the extension of the measurement range. The difference to the error terms discussed in section 5.1. is that this error has a multiplicative nature that increases with larger OPDs. Hence, in contrast to phase noise, if the interferometer is adjusted close to $OPD \approx 0$ the error introduced is rather negligible compared with the expected error when the interferometer is adjusted near to $OPD \approx UMR$ (where the error is maximal). For the example in section 3, an accurate calculation of $M_{01}^{\#}$ in Eq. (33) requires following noise criterion (error correcting property not considered), assuming $OPD < 588\ \Lambda_{01}$:

$$1/28 \geq |\, fract\,[588/S_{1,2}]\,| + 0.01 \qquad (45)$$

which can be accomplished for $S > 22866.7$. Such a value for S can be achieved with current measurement devices, provided the measurements are carried out in vacuum. For instance, the beat-wavelengths generated for the MWI system in Fig 3, give routinely a value of $S > 10^6$. Other more sophisticated systems, which extract the measurement wavelengths from a frequency comb, provide significantly higher wavelength stabilities; the system in [19] gives $S > 10^{12}$. However, these values of S, do not account for the uncertainty in the refractive index, which is the major limitation even for systems as in [19]. Popular methods for the refractive index determination are based on the Edlen formula [25] or employ frequency comb methods [26]. The obtained accuracy (standard deviation) in the refractive index is in the order of 10^{-7} [25] and 10^{-9} [26]. Hence, a typical achievable value of S for the case in Eq. (44) is $S \sim 26\,000$ and $S \sim 2\,600\,000$ assuming a totally uncorrelated uncertainty in the order of 10^{-7} [25] and 10^{-9} [26], respectively. For comparison, an uncorrelated uncertainty in the order of 10^{-7} for the measurement wavelengths in Eq. (40) for the case of Fig. 3 is equivalent to $\Delta\Lambda_{01}/\Lambda_{01} < 1.7 \times 10^{-4}$ and $\Delta\Lambda_{02}/\Lambda_{02} < 5 \times 10^{-5}$.

Once $M_{01}^{\#}$ is calculated using Eq. (15), it is possible to extend the measurement using the consideration made in Eq. (20). The noise criteria are similar to Eq. (44), but need to take into account the presence of an additional term:

$$1/q_{k,13} \geq |\, fract[\frac{U_{01}}{S_{13}} + M_{01}^{\#}\partial F_{12}]\,| + \kappa_{k,13} + 6\sigma_{R_{1,3}}, \qquad (46)$$

where $\delta F_{i,k} = |F_{i,k}^{\#} - F_{i,k}|$. For the example in section 3, an accurate calculation of $\mu_{01}^{\#}$ in Eq. (33) requires, using Eq. (46) and assuming $OPD < 588\ \Lambda_{01}$ and $M_{01}^{\#} < q_{k12}$

$$1/21 \geq |\, fract\,[\frac{588}{S_{13}} + 28\times\partial F_{12}]\,| + 0.01. \qquad (47)$$

For the case of a totally uncorrelated uncertainty in the order of 10^{-7} [25] and 10^{-9} [26], the achievable values of δF_{12} are in the order of $\delta F_{12} < 5 \times 10^{-4}$ and $\delta F_{12} < 5 \times 10^{-6}$, respectively. Similar to the case of Eq. (44), the error in Eq. (46) depends on the stability of the ratio of the beat wavelengths $F_{i,k}$. This implies that common mode errors in the calculation of the beat-wavelength have only a minor impact.

6. Discussions

The methodology presented in this work provides a different perspective on the behaviour of MWI systems and reports an error correcting nature for beat-wavelength approaches. This aspect is particularly interesting for the system design, because the choice of measurement wavelengths allow the violation of the noise criteria for a given pair of beat-wavelengths, if there is the opportunity in subsequent calculations to correct for this error. This analysis also implies that the noise criterion should not be violated, if there are no further calculations made that can correct for such an error, because this would introduce errors that reduce the MWI system reliability.

The example in section 3 shows the performance of such a strategy, where the particular choices on the measurement wavelengths have been made in order to provide an didactic example as well as a good comparison with other available approaches. The parameter F_{12} has been chosen to be $F_{12} = 95/28$. Conventional beat wavelength approaches have an $UMR = \Lambda_{01}$. Extended beat wavelength approaches [2,3] make use of the fractional part in F_{12}, and extend the UMR by a so-called gain factor g that equals g = NINT[1/|fract(F12)|] = 3. It has been shown [5,6] however, that this class of algorithms only provide a solution to a limited range of measurement wavelengths; for the case presented here when encoding the information using Eq. (15) the gain factor for the corresponding pair of beat-wavelengths (Λ_{01} and Λ_{02}) equals $g = q_k = 28$, giving an UMR equal to $UMR = 28\ \Lambda_{01}$.

The algorithm of section 2 (as well as EF and CRT approaches) indicate that there is a potential gain when using the fringe information at the other beat wavelengths, i.e. Λ_{03} for the calculation of M_{01}. It is shown in sections 2 and 3, that for the example in Fig. 3, the information contained in F_{13} increases the UMR by an additional factor of 21, $UMR = 588\ \Lambda_{01}$ - just by utilizing this fringe information. The example in section 3 also indicated that an extension of the UMR can only be made, if there is additional information available near multiples of the UMR. This behaviour is consistent with EF based approaches [11,12].

The particular choices of the measurement wavelength in Fig. 2 also pose an example where the noise criterion of Eq. (22) $6\sigma_{R1,3} \leq 1/q_{k1,3}$, is violated, but the error in the calculated value M_{01} does not propagate further in the calculation of M_{02} as it is corrected by subsequent calculations. Notably, it is possible to extend the error correcting nature of this set of wavelengths by introducing a fractional part (i.e. tuning the largest measurement wavelength) in the value of sf.

The simulation in Fig. 2 assumed solely a phase uncertainty with a standard deviation of 1/600th of a fringe. As discussed in section 5, there are additional error terms due to uncertainties of the wavelength and the refractive index. A full analysis of these errors (see [12] and section 5) requires particular knowledge of the correlation in the error between various wavelengths. Nevertheless, when assuming the case of entirely uncorrelated errors in the uncertainty of the wavelength and the refractive index at each wavelength, the set of measurement wavelengths of Fig. 2 can be employed in experimental practise, if $|\Delta\lambda/\lambda| < 2 \times 10^{-9}$. This can be achieved when using e.g. techniques based on references [19] and [26].

The example in Section 4, shows an MWI design for a significantly higher level of phase, wavelength, and refractive index uncertainties over an absolute measurement range of ~18mm. The measurement wavelengths were chosen such that $F_{12} \sim 10.5317$. The corresponding NICF of F_{12} is therefore given as $s_k/q_k = \{ 11/1; 21/2; 158/15; 495/47;$ etc.$\}$, where for the case of Fig. 4 the phase unwrapping procedure is carried out with $q_k = 2$. The measurements were subject to the wavelength uncertainty of the FBGs and the OSA as well as uncertainty in the refractive index [25], which required constant monitoring of the measurement wavelengths using multiple measurements and the use of correction factors [12,25]. The uncorrelated components of the uncertainty were estimated to give $S > 10^6$ (in vacuum) $|\Delta\lambda/\lambda| < 1 \times 10^{-6}$ (in medium). These uncertainties limited the choice in the NICF of F_{12} to $q_k = 2$ (UMR = 18.17mm) and prohibited a phase unwrapping procedure with $q_k = 15$ (equivalent to an UMR = 136.3mm). Notably, the choice of F_{12} with $|\text{fract}[F_{12}]| = 1/q_k$ is a special case of wavelength selections that employ the de Groot phase unwrapping procedure, originally developed for measurement wavelengths [2] but here applied to beat wavelengths as in reference [3]. Hence, both the algorithm presented here as well as the de Groot variant in [3] have the same UMR. However, in contrast to the approach in [3], the algorithm introduced in section 3 has the ability to use the fringe information at the beat Λ_{03} for the calculation of M_{01}. This does not increase the UMR, but provides additional system reliability.

7. Conclusions

In summary, this work introduces an algebraic solution to the phase unwrapping problem that resembles the equations of beat-wavelength approaches and allows the direct calculation of the unknown integer fringe order m_0. In contrast to beat-wavelength approaches this method exhibits the advantages of EF, i.e. a flexibility in choosing the measurement wavelengths and a robustness against noise over an extended unambiguous range. This theoretical description for multi-wavelength Interferometry provides a fundamental understanding of the relationship of wavelength combinations, phase noise and measurement distance, including the error correcting nature of the algorithm. Such a combined property has only been known for the approach in [6], however, the method reported here provides an intuitive calculation procedure with lower computational effort and lower memory requirements, making it applicable to full-field real-time measurements.

It is possible to take advantage of the error correcting nature of this algorithm by choosing specific pairs of beat-wavelengths that deliberately break the noise criterion, if there is a different pair of beat-wavelengths that correct for this deficiency. This provides higher flexibility in the choice of measurement wavelength while ensuring a high reliability.

This multi-wavelength strategy has been verified in both simulations (see Figs. 2 and 3) and experiments over an absolute measurement range of ~18mm (see Fig. 4). The experimental results show a proof of concept for ultra-high dynamic range Interferometry that is better than 1 part in 2.4×10^6. This is achieved without the need for closely separated measurement wavelengths.

The results of this work have numerous applications in absolute distance metrology [20,21,27-29], discrete wavemeters [30,31], and full-field MWI and profilometry techniques [7-9, 22, 24,32], or multi-wavelength digital holography [33-35].

A Matlab code of this algorithm can be requested from K. Falaggis (falaggis@gmx.de). He also acknowledges the support of the statutory funds of the Warsaw University of Technology.

References

1. J. C. Wyant, "Testing aspherics using two wavelength holography," Appl Opt 10, 2113–2118 (1971).
2. P. J. de Groot, "Extending the unambiguous range of two-color interferometers," Appl. Opt. **33**, 5948 (1994).
3. K. Falaggis, D. P. Towers, and C. E. Towers, "Multiwavelength interferometry: extended range metrology.," Opt. Lett. **34**, 950–2 (2009).
4. C. R. Tilford, "Analytical procedure for determine lengths from fractional fringes," Appl. Opt. **16**, 1857–1860 (1977).
5. K. Falaggis, D. P. Towers, and C. E. Towers, "Unified theory of phase unwrapping approaches in multiwavelength interferometry," in *Proc. SPIE 8011, 80117H (2011)* (2011), Vol. 8011, p. 80117L–80117L–10.
6. K. Falaggis, D. P. Towers, and C. E. Towers, "Method of excess fractions with application to absolute distance metrology: analytical solution," Appl. Opt. **52**, 5758–65 (2013).
7. V. I. Gushov and Y. N. Solodkin, "Automatic processing of fringe patterns in integer interferometers," Opt. Lasers Eng. **14**, 311–324 (1991).
8. J. Burke, T. Bothe, W. Osten, and C. Hess "Reverse engineering by fringe projection," Proc. SPIE **4778**, 312–324 (2002).
9. C. E. Towers, D. P. Towers, and J. D. C. Jones, "Time efficient Chinese remainder theorem algorithm for full-field fringe phase analysis in multi-wavelength interferometry.," Opt. Express **12**, 1136–43 (2004).
10. Benoît, R, 'Application des phénomènes d'interférence à des déterminations métrologiques', Phys. Radium, 7, 57-68. (1898).
11. K. Falaggis, D. P. Towers, and C. E. Towers, "Method of excess fractions with application to absolute distance metrology: theoretical analysis.," Appl. Opt. **50**, 5484–98 (2011).
12. K. Falaggis, D. P. Towers, and C. E. Towers, "Method of excess fractions with application to absolute distance metrology: Wavelength selection

and the effects of common error sources," Appl. Opt. **51**, 6471 (2012).
13. K. Falaggis, D. P. Towers, and C. E. Towers, "Generalized theory of phase unwrapping: approaches and optimal wavelength selection strategies for multiwavelength interferometric techniques," in J. Schmit, K. Creath, C. E. Towers, and J. Burke, eds. (2012), p. 84930O–84930O–11.
14. A. Hurwitz, "Über eine besondere Art der Kettenbruch-Entwicklung reeller Grössen," Acta Math. **12**, 367–405 (1889).
15. Falaggis, K., Towers, D. P., & Towers, C. E. (2009). Phase measurement through sinusoidal excitation with application to multi-wavelength interferometry. Journal of Optics A: Pure and Applied Optics, 11(5), 054008. doi:10.1088/1464-4258/11/5/054008
16. de Groot, P. J. (2009). "Design of error-compensating algorithms for sinusoidal phase shifting interferometry". Applied optics, 48(35), 6788–96.
17. P. de Groot, "Sinusoidal phase shifting interferometry," U.S. patent application 2008/0180679 Al (2008).
18. M. Volkov and T. Vorontsova , "Investigation of noise-immunity of the method of extending the unambiguous range in two-wavelength interferometric systems", AIP Conference Proceedings, 1537, 172-177 (2013), doi:10.1063/1.4809708
19. Kim, Y.-J., Chun, B. J., Kim, Y., Hyun, S., & Kim, S.-W. (2010). "Generation of optical frequencies out of the frequency comb of a femtosecond laser for DWDM telecommunication". Laser Physics Letters, 7(7), 522–527. doi:10.1002/lapl.201010012
20. Xuejian Wu, Haoyun Wei, Hongyuan Zhang, Libing Ren, Yan Li, and Jitao Zhang, "Absolute distance measurement using frequency-sweeping heterodyne interferometer calibrated by an optical frequency comb," Appl. Opt. 52, 2042-2048 (2013)
21. Joohyung Lee, Seongheum Han, Keunwoo Lee, Eundeok Bae, Seungman Kim, Sanghyun Lee, Seung-Woo Kim and Young-Jin Kim "Absolute distance measurement by dual-comb interferometry with adjustable synthetic wavelength", Meas. Sci. Technol. 24 045201 doi:10.1088/0957-0233/24/4/045201
22. W. Nadeborn, P. Andra, and W. Osten, "A robust procedure for absolute phase measurement," Opt. Lasers Eng. 24, 245– 260 (1996).
23. Towers, C. E., Towers, D. P., & Jones, J. D. C. (2003). Optimum frequency selection in multifrequency interferometry. Opt. Lett., 28(11), 887–9.
24. A. Pförtner and J. Schwider, "Red-green- blue interferometer for the metrology of discontinuous structures," Appl. Opt. 42, 667–673 (2003).
25. Boensch, G., & Potulski, E. (1998). Measurement of the refractive index of air and comparison with modified Edl n's formulae. Metrologia, 35(2), 133–139. doi:10.1088/0026-1394/35/2/8
26. Zhang, J., Lu, Z. H., & Wang, L. J. (2008). Precision refractive index measurements of air, N2, O2, Ar, and CO2 with a frequency comb. Applied Optics, 47(17), 3143–51.
27. Asloob Ahmad Mudassar and Saira Butt, "Displacement sensor for indoor machine calibrations," Appl. Opt. 52, 3461-3472 (2013)
28. Harry, G. M. (2010). Advanced LIGO: the next generation of gravitational wave detectors. Classical and Quantum Gravity, 27(8), 084006. doi:10.1088/0264-9381/27/8/084006
29. J. E. Decker, J. R. Miles, A. A. Madej, R.F. Siem sen, K. J. Siemsen, S. de Bonth, K. Bustraan, S. Temple, and J. R. Pekelsky, "Increasing the range of unambiguity in step-height measurement with multiple-wavelength interferometry application to absolute long gauge block measurement," Appl. Opt. 42, 5670–5678 (2003).
30. Hao Yu, Carl Aleksoff, and Jun Ni, "Accuracy of a multiple height-transfer interferometric technique for absolute distance metrology," Appl. Opt. 51, 5283-5294 (2012)
31. Carl Aleksoff ; Hao Yu; Discrete step wavemeter. Proc. SPIE 7790, Interferometry XV: Techniques and Analysis, 77900H (August 02, 2010); doi:10.1117/12.860897.
32. Towers, C. E., Towers, D. P., & Jones, J. D. C. (2005). Absolute fringe order calculation using optimised multi-frequency selection in full-field profilometry. Optics and Lasers in Engineering, 43(7),788–800.doi:10.1016/j.optlaseng.2004.08.005
33. Li Xu, Carl C. Aleksoff, and Jun Ni, "High-precision three-dimensional shape reconstruction via digital refocusing in multi-wavelength digital holography," Appl. Opt. 51, 2958-2967 (2012)
34. Dohet-Eraly, J., Yourassowsky, C., & Dubois, F. (2014). Refocusing based on amplitude analysis in color digital holographic microscopy. Optics Letters, 39(5), 1109–12. doi:10.1364/OL.39.001109
35. M. Fratz, D. Carl, "Novel Industry Ready Sensors for Shape Measurement Based on Multi Wavelength Digital Holography," Fringe 2013, Osten, Wolfgang, Conference Proceedings, Springer Berlin Heidelberg, DOI:10.1007/978-3-642-36359-7_84

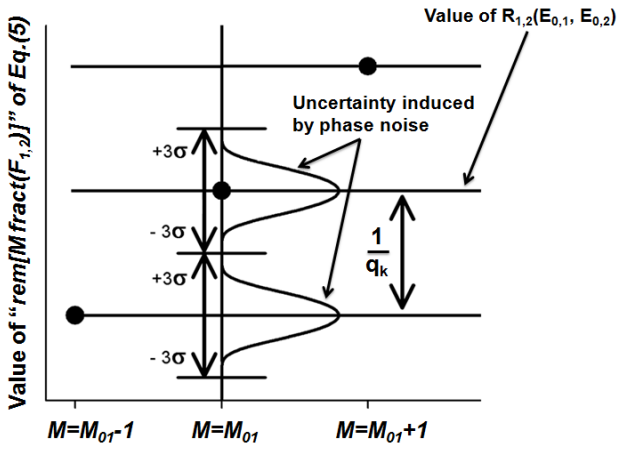

Fig. 1. Graphical representation of the uncertainty present in Eq. (7), which leads to the noise criterion in Eq. (14).

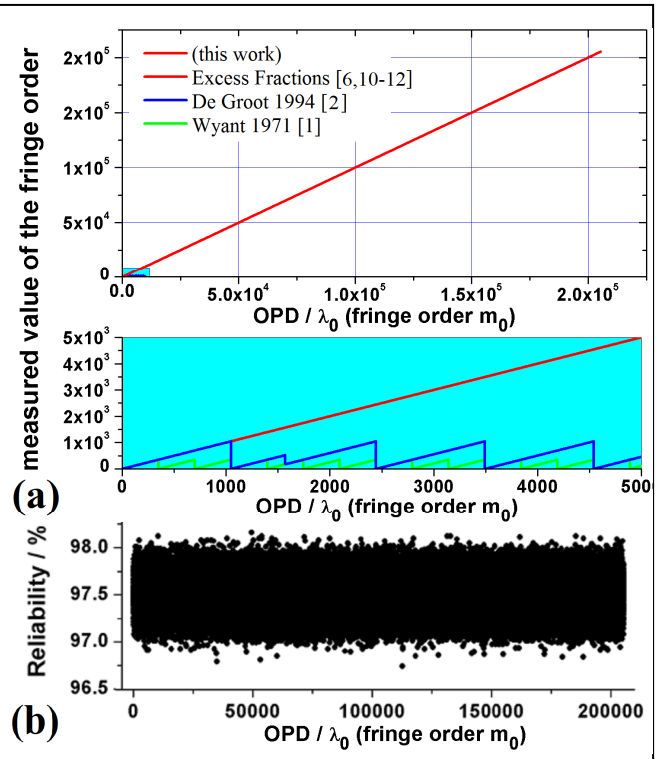

Fig. 2. (Color online) (a) UMR of a four wavelength interferometer with $sf = 23$, F_{23}=94/21, and F_{12}=95/28 over the measurement range of UMR / λ_0 = 205390 fringe orders and no noise. (b) Simulated reliability for uncorrelated AWGPN of a standard deviation of 1/600th of a fringe.

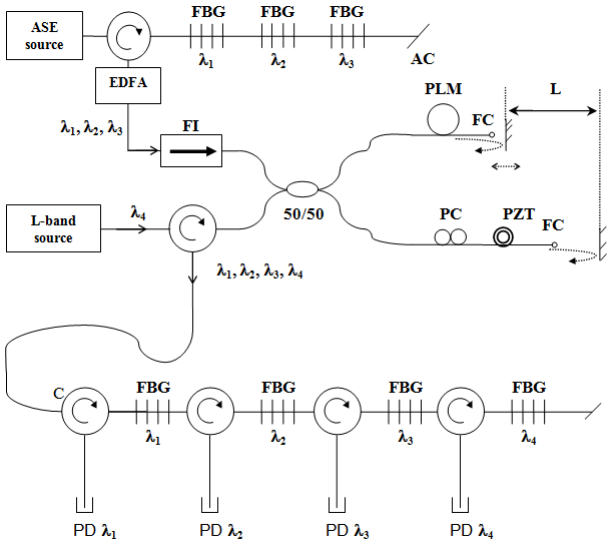

Fig. 3. Overall schematic of the fiber interferometer for four wavelength multi-wavelength interferometry. FBG – fiber Bragg grating, FI – Faraday isolator, PC – polarization controller, PZT – piezoelectric transducer, FC – fiber collimator, PD – photodiode, EDFA – Erbium doped fiber amplifier, ASE – amplified spontaneous emission source, PLM – path length matching fiber, AC – angle cleave, C – fiber circulator.

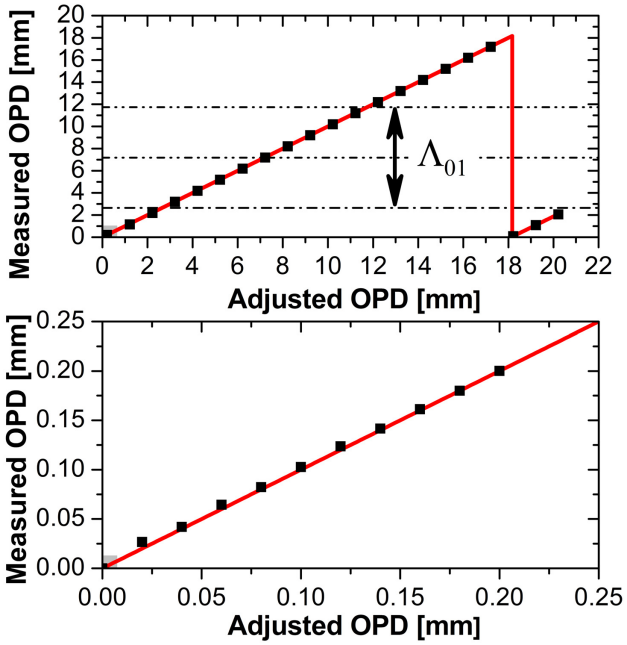

Fig. 4. (Color online) Simulated (solid red line) and measured (black squares) optical path difference using the phase unwrapping procedure of this work. The wavelengths used in the interferometer were: 1528.043, 1528.300, 1530.754 and 1595.289 nm.